Catena 207 (2021) 105701

Contents lists available at ScienceDirect

Catena

journal homepage: www.elsevier.com/locate/catena

Spatial distribution characteristics of pedodiversity and its major driving factors in China based on analysis units of different sizes

Mengyu Luo, Tianwei Wang *, Zhenyuan Li, Tieyang Zhang, Jiawei Yang, Nian Li, Zhaoxia Li

College of Resources and Environment, Huazhong Agricultural University, Wuhan 430070, China

ARTICLE INFO

Keywords:
Pedodiversity
Driving factor
Spatial distribution characteristic
China
Size

ABSTRACT

Knowledge of pedodiversity is essential for the protection and management of soil resources. The analysis of regional pedodiversity is typically based on analysis units of different sizes. However, the effect of analysis unit size on regional pedodiversity studies remains unclear. In this paper, the effects of analysis unit size on the studies of spatial distribution characteristics of pedodiversity and its major driving factor in China were studied based on two levels of geomorphological regions. A combined method encompassing the moving window, soil richness, and Shannon index was used to analyze the spatial distribution pattern of pedodiversity in China. A geographical detector was used to determine a major driving factor of pedodiversity in each geomorphological region. The spatial distribution pattern of pedodiversity based on two levels of geomorphological regions both showed that pedodiversity was highest in southern China, followed by northern China, and lowest in the Qinghai-Tibet Plateau, which indicated that analysis unit sizes had little effect on the study on spatial distribution pattern of pedodiversity. The major driving factor analysis of pedodiversity based on first-order geomorphological regions showed that the major driving factor in China, except for the Qinghai-Tibet Plateau, was parent material. However, the results based on second-order geomorphological regions showed that the major driving factors of pedodiversity, except for the Qinghai-Tibet Plateau, were parent material and topography in hilly regions, topography in mountainous regions, and parent material in regions occupied by alluvial landforms, aeolian landforms, or karst landforms. The driving factor analysis of pedodiversity based on the two levels of geomorphological regions suggested that the effect of the analysis unit sizes on the major driving factor study was significant. The results of this study are an important supplement for pedodiversity studies.

1. Introduction

Pedodiversity, also known as soil diversity, is used to explore, quantify and compare the complexity of soil patterns in different units (Amundson et al., 2015; Fu et al., 2018b; Ibáñez et al., 2014, 1995). Soil is an important component of an ecological system, and soil diversity has profound repercussions on biodiversity patterns (Ibáñez et al., 2014). Amundson et al. (2015) pointed out that “*maintaining soil diversity is important for the stability and resilience of global biogeochemical systems in the face of anthropogenic disturbances*”. Accordingly, a thorough understanding of the spatial distribution characteristics of pedodiversity and its driving factors is crucial for the protection and management of an ecological system (Fu et al., 2018b; Rannik et al., 2016).

In the 1990s, the concept of pedodiversity was defined (Ibáñez et al., 1995; McBratney, 1992). Researchers have conducted numerous studies on approaches that measure pedodiversity based on the methodologies of biodiversity, taxonomy, and landscape ecology (Ibáñez et al., 2005a, 2005b; McBratney and Minasny, 2007; Minasny et al., 2010; Pindral et al., 2020). Recently, indexes that are typically used in biodiversity and landscape ecology have become the most common approaches in pedodiversity studies (Fu et al., 2018b). Spatial patterns of pedodiversity based on these indexes have been explored at different scales. At the global scale, the pedodiversity value in an intermediate latitude climatic zone is greater than that at circumequatorial and circumboreal latitudes (Ibáñez et al., 1998). At the national scale, regions located in the transition zone from the semihumid to semiarid and arid climates have higher pedodiversity than a single climate zone (Shangguan et al., 2014). At the regional scale, pedodiversity is high in regions with higher local variety in soil-forming factors (Daněk et al., 2016). Furthermore, studies on the driving factors of pedodiversity have been conducted.

* Corresponding author.
E-mail address: wangtianwei@webmail.hzau.edu.cn (T. Wang).

https://doi.org/10.1016/j.catena.2021.105701
Received 17 March 2021; Received in revised form 5 June 2021; Accepted 25 August 2021

Previous studies have suggested that the major driving factors of pedodiversity include natural factors (e.g., topography, climate, etc.) (Fu et al., 2018b; Ibáñez and Effland, 2011; Minasny et al., 2010), anthropogenic factors (e.g., farming, construction, etc.) (Dazzi and Giuseppe, 2016, 2009; Fu et al., 2019; Papa et al., 2011; Shangguan et al., 2014), the soil classification hierarchy (Ibáñez and Effland, 2011; Shangguan et al., 2014), and the soil classification system (Gerasimova et al., 2020). However, although numerous driving factors have been studied on pedodiversity, most are still described qualitatively. Quantitative analysis of the factors is critical for an in-depth understanding of pedodiversity for use in soil protection and management (Fu et al., 2018b). In general, to data, pedodiversity research has made great progress. However, compared with biodiversity studies, pedodiversity studies have a short history and fewer researchers and achievements in the field. Therefore, it is necessary for pedodiversity to further study.

China is suitable for soil diversity research. The country includes various geomorphological types, such as plains, planforms, hill and mountains. Moreover, soil types are diverse in China. The country contains 96% of the soil types in the first-level classification of the Food and Agriculture Organization (FAO) soil classification system ([dataset] FAO/IIASA/ISRIC/ISSCAS/JRC, 2012; Li et al., 2008). Additionally, soil information is abundant in China. Soil scientists in China spent 20years conducting a national soil survey. Based on the survey results, a scientific soil database was built for China (Shi et al., 2006). The database includes 7292 soil profiles. Information for each profile in the database includes soil classification, physical and chemical properties, profile characteristics, and production capacity (Shi et al., 2010; Yu et al., 2011). China has various geomorphology types, soil types and sufficient soil data. However, the current research on soil diversity mainly focuses on regional scales such as the Henan Province, Nanjing city and the Shandong Province (Fu et al., 2019). The spatial distribution characteristics of pedodiversity and its controlling factors in China remain unclear. It is crucial to clearly understand the spatial distribution characteristics for the conservation and management of national soil resources and for promoting studies on soil diversity.

Studies on regional pedodiversity could be based on different analysis units, including climatic belts (Ibáñez et al., 1998), administrative boundaries (Amundson et al., 2003), geomorphology units (Ibáñez et al., 2015, 1998), and grids (Fu et al., 2018a; Shangguan et al., 2014). The analysis units are usually different sizes. However, when studying the spatial distribution characteristics of pedodiversity and its major controlling factor in an area, are the results obtained using different sizes of analysis units are the same or similar? The answer remains unclear. Clear knowledge of this phenomenon will be an important supplement for pedodiversity studies.

Geomorphological regionalization divides an area into several geomorphological regions based on similarities and differences in morphology, origin, and development (Wang et al., 2020). Geomorphological regionalization has typically multiple hierarchies (Li et al., 2013; Wang et al., 2020). The sizes of geomorphological regions between different hierarchies are significantly different (Li et al., 2013), which is convenient for the study of the effect of analyzing unit size on natural resource studies. Additionally, by way of integrating the factors of parent material, relief, time, and surface processes, the geomorphic environment constitutes an essential part of the spatial and temporal framework in which soils originate, develop, and evolve (Zinck, 2013). Therefore, by considering multiple hierarchies of geomorphological regions and the relationship between geomorphology and soil formation, this soil diversity study was conducted based on geomorphological regions. The objectives of this study were to 1) determine the spatial distribution characteristics of pedodiversity and its major driving factor in China based on first-order geomorphological regions and second-order geomorphological regions, respectively, and 2) analyze the effects of the size of the analysis units on the studies of spatial distribution characteristics of pedodiversity and its major driving factor.

2. Study area

China with a total area of approximately 9,600,000 km^2 (73°40′-135°05′ E, 3°58′-53°31′ N) is located in the southeast of the Eurasian continental plate, with the western Pacific and Philippine plates to the east and the Indian plate to the southwest (Ren et al., 1999; Wang et al., 2020). Influenced by the interactions of these plates, China includes various geomorphological types, such as plains, platforms, hills and mountains (Li et al., 2008). Specifically, the areas of plains, platforms and hills account for 25.48%, 10.83% and 20.27% of the total area of China, respectively. These geomorphological types are mainly distributed in northern China. Mountains are mainly distributed in southern China and its area accounts for 43.43% of the total area in China (Editorial committee of geomorphological atlas of the people's republic of China, 2009). Parent material types in China contain igneous material, metamorphic material, sedimentary material, and unconsolidated materials formed by the transport of water and wind (Zhang, 2002). The unconsolidated materials in China are mainly distributed in plateaus and plains north of 30°N (Liu and Yuan, 1985) (Fig. 1c).

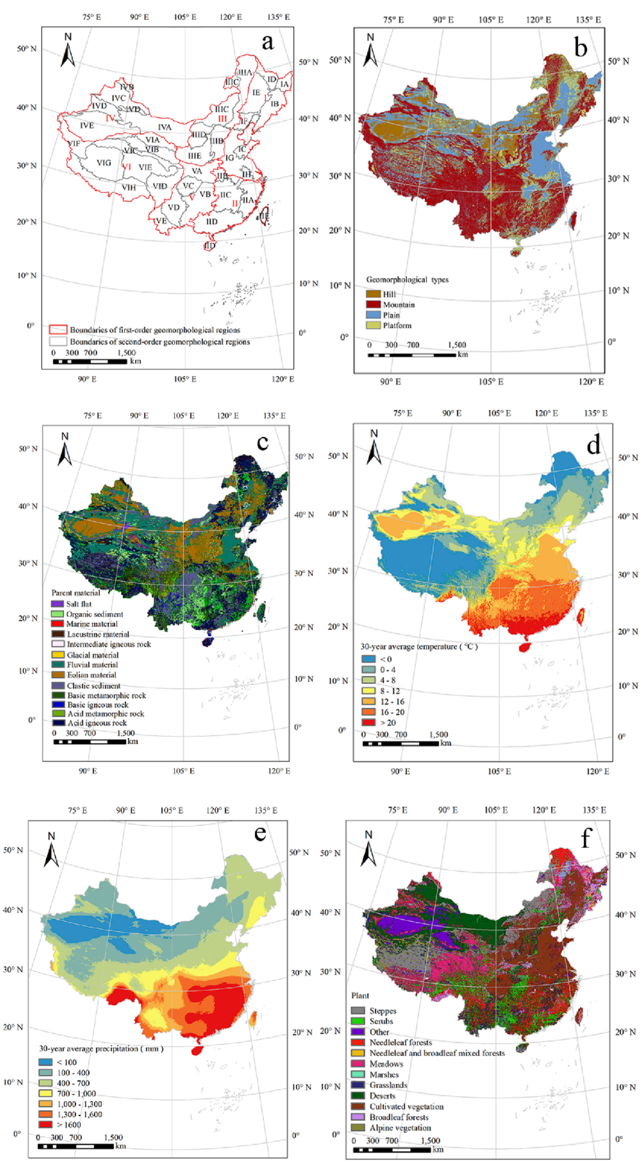

Fig. 1. Map depicting environmental factors and two-level geomorphological regions in China. The abbreviations of geomorphological region are shown in Table 1 and Table 2.

The 30-year average temperature from 1980 to 2010 in eastern China gradually decreased from south to north (Fig. 1d) (Zhang, 2002). The annual average temperature is above 22 °C in southeastern China, 12–14 °C in middle-eastern China, and below 0 °C in the northern region of northeastern China. The temperature in the arid basins of northwestern China is approximately the same as the average temperature in middle of eastern China. The lowest average temperature is found on the Qinghai-Tibet Plateau (Fig. 1d). Precipitation in eastern China is influenced by the Pacific Ocean and richer than that in western China. The 30-year average precipitation from 1980 to 2010 is 1600 mm in southeastern China, while it is only 200 mm in northwestern China. Precipitation in the Tarim and Tsaidam basins is less than 50 mm due to the influence of topography (Fig. 1e) (Zhang, 2002). Climate diversity implies the diversity of plant types in China. The vegetation in China is divided into zonal vegetation and interzonal vegetation. Zonal vegetation is directly related to climate condition. There are coniferous forests in the cold-temperate region, coniferous and broad-leaved mixed forests in the temperate region, deciduous broad-leaved mixed forests in the warm-temperate region, evergreen broad-leaved forests and deciduous broadleaf mixed forests north of the subtropical region, evergreen broad-leaved forests in the middle of the subtropical region, monsoonal forests of the subtropical region, and monsoonal forests and rainforests in the tropical region. Interzonal vegetation includes meadows and marshes and is distributed throughout the country. (Fig. 1f) (Wu, 1995; Zhang, 2002).

3. Materials and methods

3.1. Data sources

To analyze spatial distribution characteristics of pedodiversity and its major driving factors in each geomorphological region, the data required in this study include soil data, geomorphological region data and 5 factor data controlling pedodiversity that consist of climate, parent material, plant, topography and anthropogenic activity. Notably, the time factor was not considered in this study because the soil-forming time in each geomorphological region may be relatively uniform (Wang et al., 2020). With reference to previous studies, the 5 factors controlling pedodiversity were represented by 9 factors that consisted of 30-year average precipitation and temperature from 1980 to 2010, the Shannon index of parent material, the Shannon index of plants, percent of farmland, the Shannon index of the positive and negative terrain, mean elevation, elevation range and variation coefficient of elevation (Fu et al., 2019, 2018b; Ibáñez and Effland, 2011; Minasny et al., 2010).

The soil data used were from Harmonized World Soil Database ([dataset] FAO/IIASA/ISRIC/ISSCAS/JRC, 2012), where soils are divided into 28 categories based on FAO-90 soil classification system (the classification system complied by Food and Agriculture Organization of the United Nations in 1988). The database covers the whole world. Soil data in China were clipped from this database using ArcMap 10.2. Geomorphological region data were acquired from the study by Wang et al. (2020), which divided landforms in China into 6 first-order geomorphological regions and 36 second-order geomorphological regions. In this study, we did not consider geomorphological region IIE due to the lack of soil data. Topographic data that consisted of the positive and negative terrain, mean elevation, elevation range and variation coefficient of elevation were derived from the digital elevation model (DEM) with a spatial resolution of 90 m. Parent material data were acquired from the Soil and Terrain database. 30-year meteorological data from 1980 to 2010, including precipitation and temperature, are spatial interpolation data based on approximately 2400 automatic weather stations in China. Vegetation data were obtained from the digital vegetation atlas of China. The effect of human activities was expressed in terms of the percent of farmland in this study. The percent of farmland was calculated in the land use type obtained from Landsat TM images for 1990 by the visual interpretation method.

3.2. Methods

In this study, first, the moving window technique (Behrens et al., 2009) and richness index were used to determine an optimal analysis window in each geomorphological region (Forman, 1995; Fu et al., 2018). The optimal analysis window and Shannon index were used to calculate pedodiversity in each geomorphological region. Then, the major driving factor of pedodiversity for each geomorphological region was found using a geographical detector (Wang et al., 2010). The effects of analysis units of different sizes on the spatial distribution characteristics of pedodiversity and its major driving factors were analyzed. The flow chart for this study is presented in Fig. 2.

3.2.1. Pedodiversity calculation in each geomorphological region

Pedodiversity in each geomorphological region was determined by combining the Shannon index and a moving window technique with richness. First, the moving window technique and richness index were used to determine an optimal analysis window in each geomorphological region. Then, pedodiversity in each geomorphological region was calculated based on the window and the Shannon index. The Shannon index was calculated as follows:

$$Shannon\ \ index = -\sum_{i=1}^{n} p_i.Inp_i \tag{1}$$

where n is richness and refers to the number of soil types and $p_i$is the proportion of the area of the ith soil type to the total area in a study area.

The procedures for selecting the optimal analysis windows are described as follows:

① Fitting a richness and area curve in each geomorphological region. In Fragstats software (version 4.2), soil richness was calculated at different window sizes based on the moving window technique (Behrens et al., 2009). In this study, 20 window sizes (from 5 km in length to 100 km in increments of 5 km) were set to fit a richness and area curve in each geomorphological region. Based on the richness results and window areas, in Origin software (version 2020), the richness-area relationship was described by a logarithmic function or power function (Ibáñez et al., 2005b). The best fitting function of the

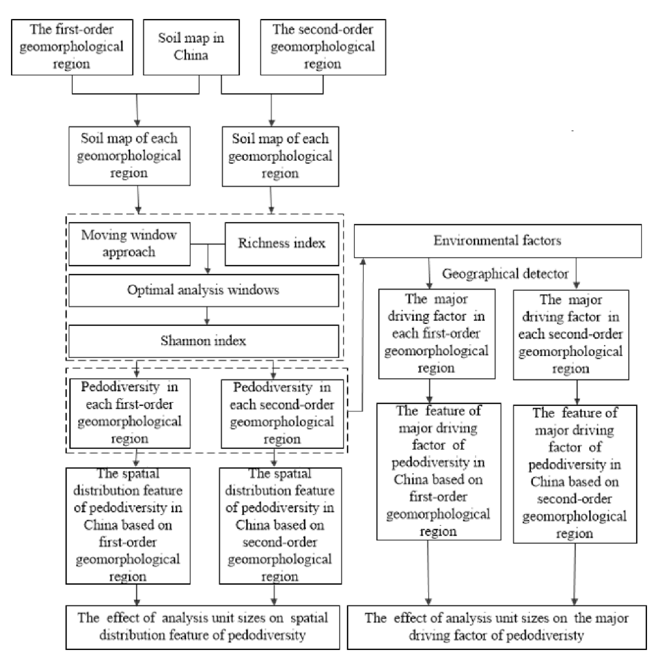

Fig. 2. Flow chart for this study.

richness-area relationship was selected by the determination coefficient of the model (R^2) (Fu et al., 2018b).

$$Logarithmic\ function:\quad S = alog(A) + b \tag{2}$$

$$Power\ function:\quad S = aA^b \tag{3}$$

where A is a window area; S is the soil richness in window area A; and a and b are fitted parameters.

② Determination of an optimal analysis window in each geomorphological region. Recent studies have indicated that biodiversity and pedodiversity have similar patterns, such as diversity-area relationships. (Ibánez and Feoli, 2013). Therefore, in this study, the method for determining an optimal sampling area in biodiversity was used to determine an optimal analysis window for pedodiversity study. In ecology, the optimal sampling area (equivalent to the optimal analysis window in this study) could be inferred from the fitted richness-area curve. Corresponding with the above richness-area curves, optimal analysis windows were listed as follows (Liu et al., 1998).

$$A_l = \frac{exp(rs_t - b)}{a} \tag{4}$$

$$A_P = \left(\frac{rs_t}{a}\right)^{1/b} \tag{5}$$

where A_l and A_p refer to the optimal analysis windows corresponding to logarithmic and power functions, respectively; S_t refers to richness in the maximum analysis window, which could be estimated by using the extrapolation method based on the species-area relationship (Palmer, 1990); a and b are fitted parameters; r ($0 < r < 1$) is the proportion of soil richness in the maximum analysis window. R values were usually chosen from 0.6 to 0.9 (Kong et al., 2016). Considering both the efficiency and accuracy of the research effort, the r value was set to 0.7 in this study.

In this study, considering the comparability of pedodiversity among first-order geomorphological regions and the efficiency and accuracy of the research effort, we selected the largest optimal analysis window of 6 first-order geomorphological regions as the analysis window for all first-order geomorphological regions. The above method was also used to select an optimal analysis window for all second-order geomorphological regions.

3.2.2. *Descriptive analysis of pedodiversity*

Pedodiversity in China was subjected to descriptive analysis with R. The mean, minimum, maximum, standard deviation, and coefficient of variation for pedodiversity were calculated to describe the data characteristics.

3.2.3. *Determining the major driving factor of pedodiversity*

The geographical detector was used to explore the major driving factor of pedodiversity in each geomorphological region. The geographical detector consists of a factor detector, ecology detector, risk detector, and interaction detector (Wang et al., 2010). However, in our study, we used only the factor detector and ecology detector. The factor detector was utilized to quantify the explanatory degree of an environmental factor for pedodiversity. An ecological factor was used to verify whether the effects of environmental factors on pedodiversity were significantly different. The combination of the factor detector and ecology detector could be used to find the major driving factor of pedodiversity.

The core idea of a factor detector suggests that if a significant spatial consistency exists between pedodiversity and its controlling factors, then an association is present between them (Wang et al., 2010). We assume that A is a controlling factor of pedodiversity. Region M is stratified into several sub-regions by A, which is denoted as a_1, a_2 and a_3

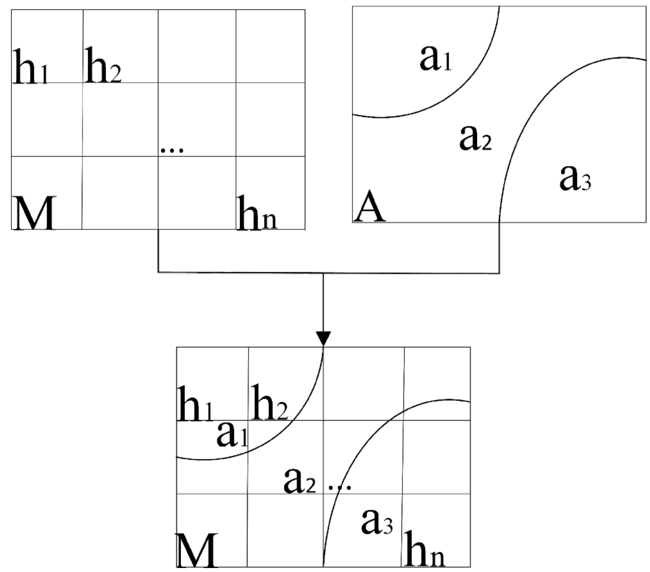

Fig. 3. Pedodiversity layer M and spatial pattern of driving factor A in the study regions M.

(Fig. 3). The spatial consistency between pedodiversity in region M and the controlling factor A is measured using the total variance in pedodiversiy and the variance in pedodiversity in each sub-region. The total variance is measured based on the observation points (h_1, $h_2 \ldots h_n$). The variance in each sub-region is measured based on the observation points within the sub-region. If the spatial distribution of peododiversity in region M is fully controlled by A, the variance sum of the three sub-regions (a_1, a_2, a_3) equals zero. Otherwise, the total variance in pedodiversity is the variation sum of the three sub-regions. A high spatial consistency suggests an environmental factor has a strong effect on pedodiversity. It is measured by q. The equation of q is described as follows.

$$q = 1 - \frac{\sum_{i=1}^{n} \sigma_i^2 N_i}{N\sigma^2} \tag{6}$$

where q denotes explanatory degree of an environmental factor for pedodiversity; n represents the number of sub-region; σ_i^2 is the internal variation in the ith sub-region; σ^2 denotes variance in the study area; N_i and N denote the number of observation in ith subregion and that in the whole study area, respectively.

The ecology detector uses the F-value test to explore whether the effects of the environmental factors on pedodiversity are significantly different. The equation of F is described as follows.

$$F = \frac{N - M}{M - 1}\frac{Q}{1 - Q} F(M - 1, N - M; \xi) \tag{7}$$

$$\xi = \frac{\left[\sum_{j=1}^{M} Y_j^2 - \frac{1}{N}\left(\sum_{j=1}^{M} Y_j \sqrt{N_j}\right)^2\right]}{\sigma^2} \tag{8}$$

where M is the number of sub-regions, N is the number of observations, and ξ is the non-central parameter; Y_j is the mean value of observations within the jth sub-region of variable. N_j is the number of observations within the jth sub-region; σ^2 denotes variance in the study area. Thus, with the given significant level, the null hypothesis H_0: $\sigma_i^2 = \sigma^2$ can be tested by checking $F(M-1, N-M; \xi)$ in the distribution table.

The geographical detector model required that an independent factor is a discrete type (Wang et al. 2010). Factors of continuous type in this study were divided into 15 levels using the approach of a natural break in GIS, with reference to the method of data discretization proposed by Wang et al. (2010).

4. Results

4.1. Optimal analysis window in the first-order and second-order geomorphology regions

The soil richness of each geomorphological region increased with window size. However, the rates of increase were different. At first, the soil richness drastically increased with window size but gradually increased when the window area exceeded a particular value (Fig. 4a1, a2). For the richness-area relationships in all geomorphology regions, R^2 for the power curve was greater than that for the logarithmic curve (not shown). Therefore, the best fitting functions for the richness-area relationship in all geomorphology regions were power curves. The ranges of the optimal analysis window lengths were 41 km to 45 km in the first-order geomorphological regions, and 26 km to 35 km in the second-order geomorphological regions (Fig. 4b1, b2). To ensure the comparability of pedodiversity values, a window with a length of 45 km length was chosen as the optimal analysis window in each first-order geomorphological region, and a window with a length of 35 km length was chosen as the optimal analysis window for each second-order geomorphological region.

4.2. Descriptive analysis of pedodiversity in China

The mean Shannon index and mean soil richness in China using the first-order geomorphological regions as spatial units were 0.92 and 4.87, respectively, which were higher than those using the second-order geomorphological regions as spatial units. However, the results of the coefficient of variation showed the opposite trend. The coefficients of variation of Shannon index and soil richness in China were 17% and 14% using the first-order geomorphological regions as spatial units, respectively. However, they were 25% and 22% using the second-order geomorphological regions as spatial units, respectively (Table. 3).

4.3. The spatial distribution pattern of pedodiversity and the relationship between pedodiversity and elevation in China

Based on first-order geomorphological regions, the Shannon indexes in geomorphological regions V and II were 1.12 and 1.04, respectively.

Table 1
Name, code and area of each geomorphological region in first-order geomorphological regions.

Codes	Names	Areas (km^2)	Codes	Names	Areas (km^2)
I	Eastern China plainslow-mountains-hills region	1,443,320	II	Southeastern China low mountains-hills-plains region	1,135,003
III	Northern China-eastern inner Mongolia middle mountains-plateaus region	1,361,987	IV	Northwestern China high and middle mountains-basins-plateaus region	1,726,160
V	Southwestern China middle and low mountains -plateaus-basins region	1,183,367	VI	Tibetan Plateau high and extremely high mountains-basins-valleys region	2,642,041

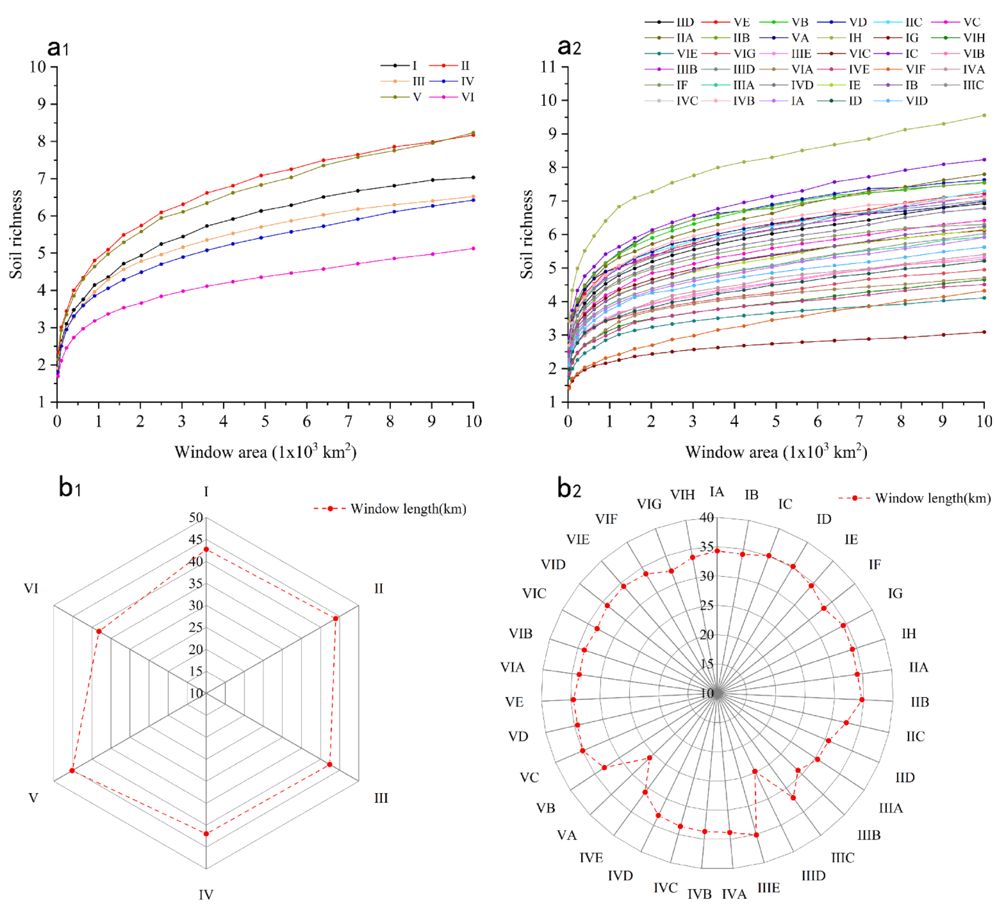

Fig. 4. The curves of window area against soil richness (a_1 and a_2) and optimal analysis windows (b_1 and b_2) in the first-order (a_1 and b_1) and second-order (a_2 and b_2) geomorphological regions. The abbreviations of geomorphological region are shown in Table 1 and Table 2.

Table 2
Name, code and area of each geomorphological region in second-order geomorphological regions.

Codes	Names	Areas (km^2)	Codes	Names	Areas (km^2)
IA	Wanda Mt and Sanjiang Plain low mountains and hills region	89,485	IB	Changbai middle and low mountains, platforms and hills region	245,884
IC	Eastern Shandong low mountains, hills and plains region	87,929	ID	Xiao Hinggan low mountains, hills and platforms region	117,708
IE	Songhua River-Liaohe River plains region	336,232	IF	Yanshan and western Liaoning low mountains, hills and platforms region	88,620
IG	Northern and eastern China plains region	431,203	IH	Ningzhen plains, hills and mounds region	46,260
IIA	Zhejiang and Fujian middle and low mountains and hills region	254,092	IIB	Huaiyang low mountains, hills and mounds region	87,671
IIC	Middle reaches of Yangtze River low mountains, hills, plains and basins region	338,884	IID	Southern China low mountains, hills and plains region	418,014
IIE	Taiwan plains and mountains region	36,341	IIIA	Da Hinggan middle and low mountains region	361,090
IIIB	Shanxi middle and low mountains and basins region	195,470	IIIC	Northeastern Inner Mongolia high plains region	348,867
IIID	Ordos Plateau and Hetao plains region	176,840	IIIE	Loess Plateau region	279,721
IVA	Inner Mongolia, Gansu and Xinjiang plateaus and plains region	569,954	IVB	Altai high and middle mountains region	46,302
IVC	Junggar basin region	287,081	IVD	Tianshan high mountains and basins region	237,892
IVE	Tarim basin region	584,932	VA	Qinling-Daba middle and low mountains region	246,905
VB	Hubei-Guizhou-Yunnan middle and low mountains region	388,456	VC	Sichuan basin region	144,456
VD	Southwestern Sichuan and central Yunnan plateaus, middle and low mountains and basins region	251,596	VE	Southwestern Yunnan middle and high mountains region	151,954
VIA	Altun and Qilian Mts high mountains and valleys region	203,661	VIB	Qaidam basin and Yellow river-Huangshui River high mountains and basins region	227,679
VIC	Central and eastern Kunlun high mountains region	235,238	VID	Hengduan high mountains and valleys region	317,963
VIE	Sources of Three Rivers high hilly mountains and plateaus-upper reaches of rivers mountains and valleys region	414,076	VIF	Karakorum and western Kunlun high and extremely high mountains region	219,820
VIG	Qiangtang Plateau lakes and basins region	503,060	VIH	Himalayan high and extremely high mountains region	520,543

Table 3
Statistical analysis of pedodiversity in China base on first-order and second-order geomorphological regions. Min denotes minimum value; Max denotes maximum value; Std denotes standard deviation; CV denotes coefficient of variation.

Regions	Index	Min	Max	Mean	Std	CV (%)
First-order geomorphological regions	Shannon index	0.68	1.12	0.92	0.16	17
	Soil richness	3.66	5.74	4.87	0.69	14
Second-order geomorphological regions	Shannon index	0.29	1.24	0.85	0.22	25
	Soil richness	2.25	6.83	4.35	0.97	22

The values were higher than the pedodiversity values in other geomorphological regions, which suggested that soil diversity in southern China (referring to geomorphological regions V and II) was generally higher in northern China (including geomorphological regions IV, III, and I (Zhang, 2019)). The pedodiversity in the Qinghai-Tibet Plateau was 0.68, which was the lowest pedodiversity in China (Fig. 5a1).

Southern China included nine second-order geomorphological regions (VA, VB, VC, VD, VE, IIA, IIB, IIC, and IID), where pedodiversity values in all regions except geomorphological region IID were higher than 0.95 (Fig. 5a2). There were 18 second-order geomorphological regions in the northern part of China. However, only four second-order geomorphological regions had pedodiversity values higher than 0.95. Pedodiversity values in most second-order geomorphological regions in the northern part of China were lower than 0.85, and the lowest pedodiversity was 0.55 (Fig. 5a2). Five of eight regions in the Qinghai-Tibet Plateau had a pedodiversity value below 0.70. The highest pedodiversity value was 0.80, and the lowest pedodiversity value was 0.29 in the Qinghai-Tibet Plateau (Fig. 5a2). Accordingly, based on the second-order geomorphological regions, pedodiversity in southern China was higher than that in northern and that in the Qinghai-Tibet Plateau was lowest (Fig. 5a2), which suggested that the characteristics of the pedodiversity spatial distribution based on analysis units of different sizes had a similar spatial pattern.

In the first-order geomorphological regions, pedodiversity in China generally increased as elevation decreased. But the two fitted models of pedodiversity in the first-order geomorphological region were not statistically significant (Fig. 5b1). In the second-order geomorphological regions, the pedodiversity trend with the change in elevation was the same as that in the first-order geomorphological regions. For the fitted models, R^2 was 0.42 for the linear model and R^2 was 0.43 for the polynomial model (Fig. 5b1). The two models were statistically significant, which suggested that the pedodiversity-elevation relationship in China based on the second-order geomorphological regions could be described by the polynomial model.

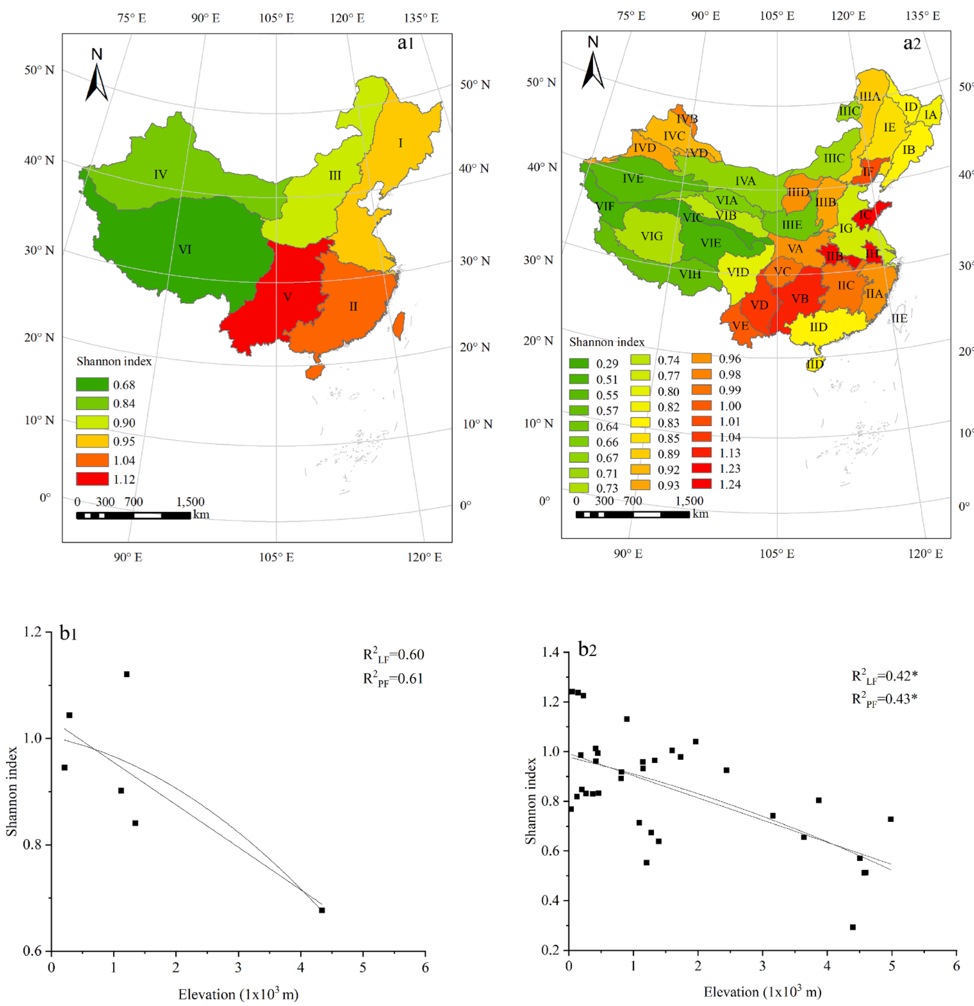

Fig. 5. Map depicting spatial distribution of the Shannon index in China based on the first-order (a_1) and second-order geomorphological regions (a_2) and the fitted linear model and polynomial model of pedodiversity against elevation in China based on the first-order (b_1) and second-order geomorphological regions (b_2). LF denotes linear model. PF denotes polynomial model. * indicates the fitted models is statistically significant at $p < 0.05$. The abbreviations of geomorphological region are shown in Table 1 and Table 2.

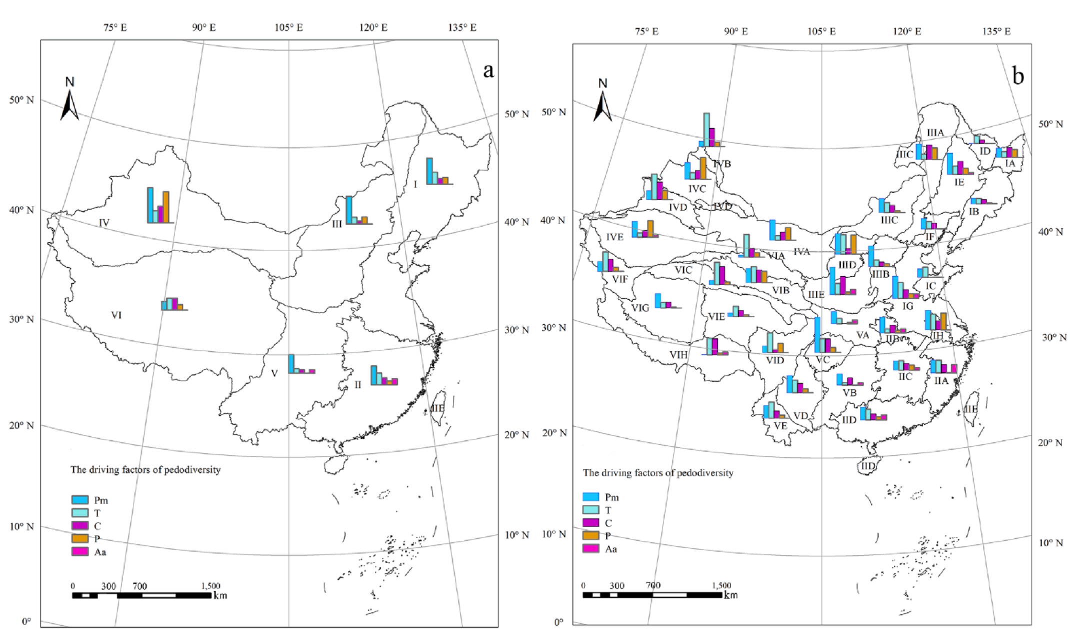

Fig. 6. Map depicting the driving factors of pedodiversity in the first-order (a) and the second - order geomorphological regions (b). Pm denotes parent material; P denotes plant; T denotes topography; C denotes climate; Aa denotes human activity. The abbreviations of geomorphological region are shown in Table 1 and Table 2.

4.4. Major driving factor identification in China based on different analysis units

In the first-order geomorphological regions, the factor detector results showed that in the Qinghai-Tibet Plateau, the explanatory degrees of topography and climate for pedodiversity were 16.99% and 16.92%, respectively, and these values were higher than those of other environmental factors (Figs. 6a, 7, 8). The results of the ecology detector showed that the explanatory degrees of topography and climate to pedodiversity were not significantly different (Fig. 8), which suggested that the major driving factors of pedodiversity in the Qinghai-Tibet Plateau were topography and climate. In the first-order geomorphological regions, parent material was the major controlling factor on pedodiversity in regions I, II, III, IV, and V. The explanatory degrees of parent material in geomorphological regions I, II, III, V, and IV were 37.66%, 27.03%, 39.85%, 50.84%, and 27.11%, respectively (Figs. 6a, 7). In terms of statistics, these values were significantly higher than the explanatory degrees of other environmental factors (Fig. 8). In the second-order geomorphological regions of the Qinghai-Tibet Plateau, the q values in region VIG were distributed as follows: parent material (29.73%) > climate (12.34%) > topography (11.76%) > vegetation (1.78%) (Fig. 7). The results of the ecology detector showed that the influence of parent material on pedodiversity was significantly higher than that of other environmental factors (Fig. 8), which suggested that the major driving factor for pedodiversity in geomorphological region VIG was different from that in the Qinghai-Tibet Plateau based on first-order geomorphological regions. The difference between the major driving factors based on the first-order geomorphological regions and those on the second-order geomorphological regions also occurred in the following regions: VE, IVD, IVB, IIC, IIA, IC, IB, ID, IIID, VIA, VIB, VIC, VID, and VIE. Topography was the major controlling factor of pedodiversity in geomorphological regions VE, IVD, IVB, ID, VIA, VIB, VIC, VID, and VIE (Figs. 6b, 7). The explanatory degrees of topography were significantly higher than the explanatory degrees of other

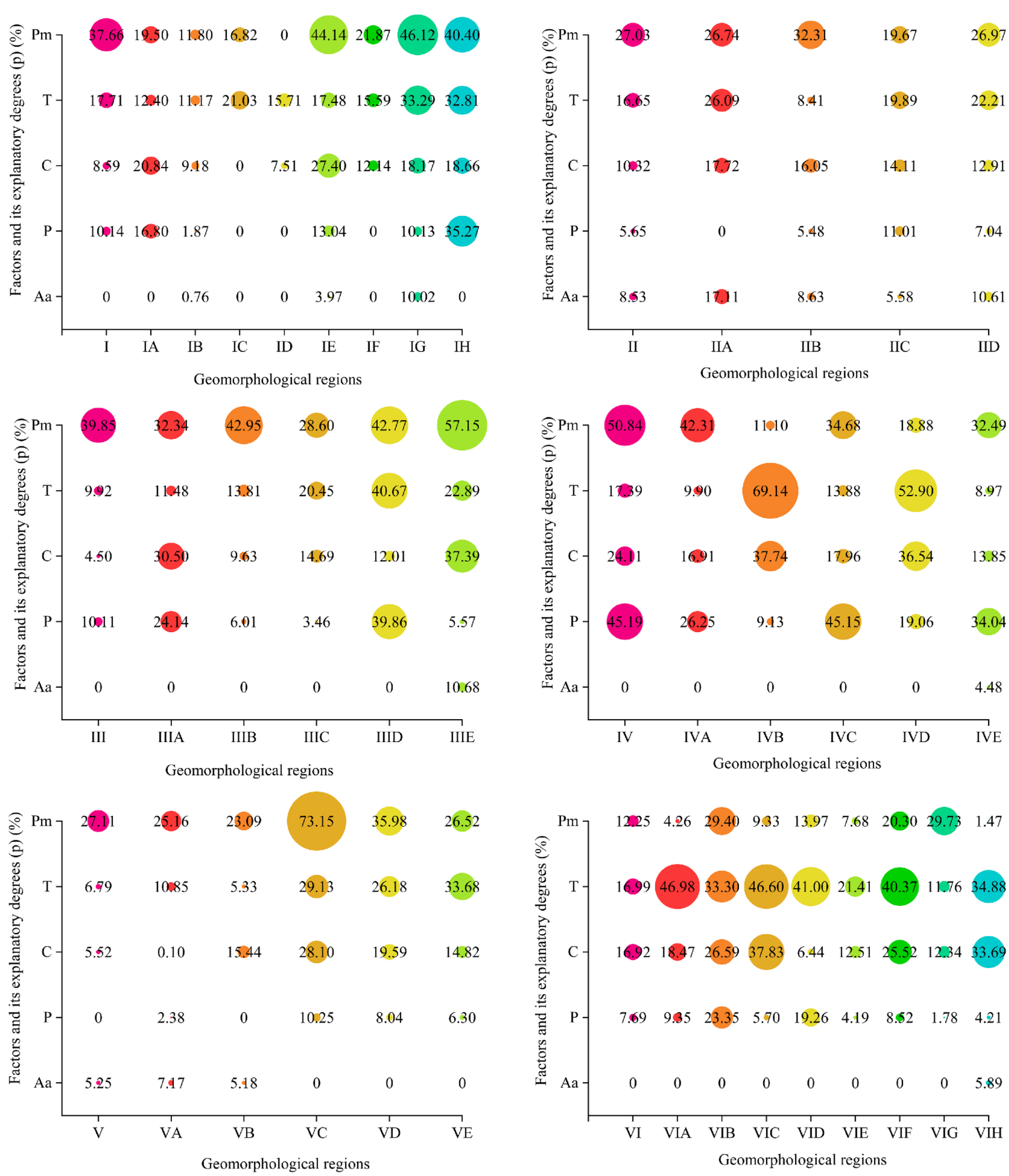

Fig. 7. Explanatory degree of environmental factors for pedodiversity in each geomorphological region. Pm denotes parent material; P denotes plant; T denotes topography; C denotes climate; Aa denotes human activity. 0 indicates that the effect of environmental factor on pedodiversity is not significant in statistics. The abbreviations of geomorphological region are shown in Table 1 and Table 2.

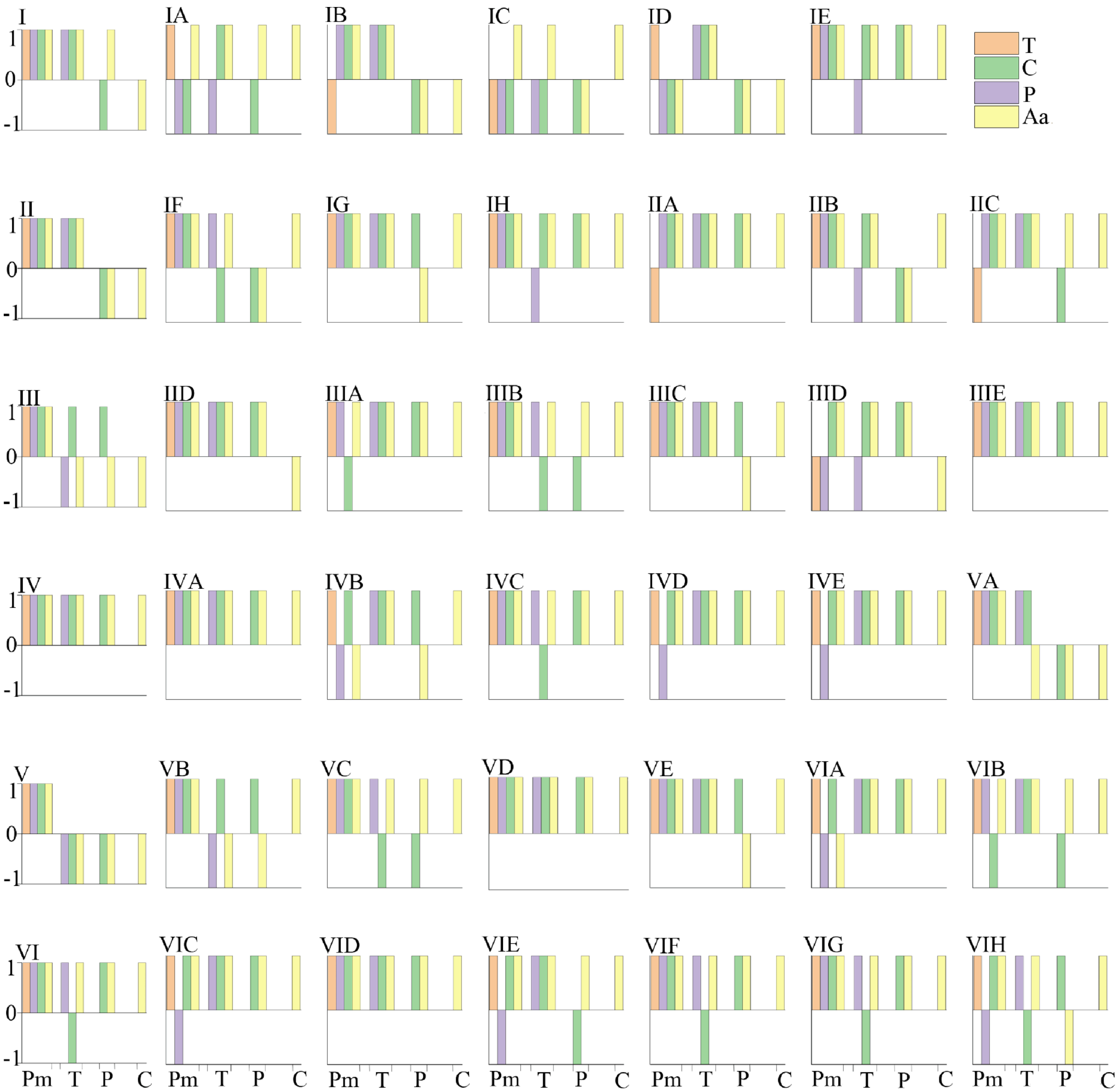

Fig. 8. The results of ecology detector in each geomorphological region. 1 indicates that the effects of environmental factors on pedodiversity are significantly different. −1 indicates that the effects of environmental factors on pedodiversity are not significantly different. Pm denotes parent material; P denotes plant; T denotes topography; C denotes climate; Aa denotes human activity. The abbreviations of geomorphological region are shown in Table 1 and Table 2.

environmental factors (Fig. 8). The q values of parent material and topography in geomorphological regions IIC, IIA, IC, IB, and IIID were not significantly different and were significantly higher than those of other environmental factors, which suggested that parent material and topography were both the major driving factors in regions IIC, IIA, IC, IB, and IIID (Figs. 6b, 7, 8). The differences between the major driving factors of pedodiversity in China based on the first-order geomorphological regions and those in the second-order geomorphological regions implied that the controlling factors of pedodiversity were dependent on the size of the analysis unit.

5. Discussion

5.1. The spatial distribution patterns of pedodiversity in China

Complex soil-forming environment produce high pedodiversity (Fu et al., 2018b). Soil diversity in southern China was higher than that in northern China, and pedodiversity in the Qinghai-Tibet Plateau was lowest (Fig. 5a, b). This result is because the soil-forming environment in southern China, including topography, parent material and climate, is more complex than that in northern China. (Zhang, 2002). In terms of topography, approximately 67% of the area in southern China consists of mountains and approximately 80% of the area in northern China is comprised of plains and plateaus (Editorial committee of geomorphological atlas of the people's republic of China, 2009). For climate, the average temperature in southern China is at least 3 times higher than that in northern China, and precipitation is 1.3 times higher (Zhang, 2002). In addition, the difference in parent material types between northern and southern China is also significant. There is a large area of alluvial deposits and aeolian deposits in northern China (Liu and Yuan, 1985). Based on the FAO-90 soil classification system, soil formed in alluvial deposits is defined as Fluvisols, and soil developed in aeolian deposits in an arid climate is defined as Arenosols (FAO/Unesco, 1997). In summary, the more complex soil-forming factors in southern China compared with northern China suggest that pedodiveristy in southern China is higher than that in northern China.

Two characteristics in the Qinghai-Tibet Plateau indicate that the soil diversity in the area was the lowest in China (Fig. 5a, b). First, the

Qinghai-Tibet Plateau is the youngest plateau in the world, and its soil development time is shorter than that in other regions in China (Chen et al., 1981). Before the Triassic period, the Qinghai-Tibet Plateau was an ocean. However, due to the extrusion of the Indian Ocean plate and the Eurasian Plate in the early Quaternary period, the Qinghai-Tibet Plateau with an average elevation over 4000 m was formed (Chen et al., 1981). Subsequently, rocks on the Qinghai-Tibet Plateau slowly weathered to form soil. Second, the Qinghai-Tibet Plateau has a low average temperature than that in other regions in China. The average temperatures in the Qinghai-Tibet Plateau are 3 °C −10 °C in the warmest month and −20 °C in the coldest month (Gong et al., 2007; Minasny et al., 2010). Two characteristics with a low average temperature and short soil development time determine that the soil of the Qinghai-Tibet Plateau has a weak development degree (Gong et al., 2007). Soil survey suggest that the areas of two young soils (Leptosols and Cambosols) occupy 70% of the area of the Qinghai-Tibet Plateau ([dataset] FAO/IIASA/ISRIC/ISSCAS/JRC, 2012), which causes the soil diversity in the Qinghai-Tibet Plateau to be lowest in China.

5.2. The major driving factor of pedodiversity in China

The simultaneous existence of soils in different developmental stages and the presence of intrazonal soils were the most important contribution to pedodiversity (Gracheva, 2011). There are 27 soil types in China based on the FAO-90 soil classification system in China, where 16 soil types are intrazonal. Parent material, underwater, anthropogenic activity, and other factors determine 8, 5, 1, and 2 intrazonal soil types, respectively (FAO/Unesco, 1997; Wilson, 2019), which implies that parent material is more likely than other factors to control the soil diversity of a region with many intrazonal soil types. Parent material gradually develops into a mature soil type through the processes of calcium removal, desalination, and desilication (Simonson, 1959). From a spatial perspective, the processes usually exist simultaneously, even in the same climate, which produces soils in different stages of development (Wu and Gong, 1983). At a regional scale, topography and parent material control soil development (Zhang, 2002). Topography indirectly influences soil development by controlling climate and soil erosion. In contrast, parent material directly controls soil development by influencing soil properties. The physical and chemical properties of soil formed in different parent materials usually show extensive differences (Tazikeh et al., 2017; Wilson, 2019), which may cause soils to be defined as different soil types based on FAO-90 soil classification system. The influences of parent material and topography on soil development and intrazonal soil types suggested that they are essential for controlling soil diversity.

There are many intrazonal soils and soils that are in different stages of development in China. The intrazonal soils are mainly distributed north of latitude 30 in China, except on the Qinghai-Tibet Plateau ([dataset] FAO/IIASA/ISRIC/ISSCAS/JRC, 2012). North of latitude 30, except for the Qinghai-Tibet Plateau, the parent materials for all geomorphological regions, except VA, VC, IC, IB, ID, IIIA, IVB, and IVD, mainly consist of alluvial deposits and aeolian deposits (sand deposits and loess) (Liu and Yuan, 1985)(Fig. 1c). Based on the FAO-90 soil classification system, soils developed in alluvial deposits and sand deposits are defined as intrazonal soils (FAO/Unesco, 1997). Soil types formed in loess were controlled by climate. However, the climate in each geomorphological region was approximately the same (Gao et al, 2019). Accordingly, the major driving factors of pedodiversity in the geomorphological regions was parent material (Figs. 6a, 7, 8).

Soil south of latitude 30 and the IC, IB, ID, IIIA, IVB, IVD, VA and VC geomorphological regions mainly consist of soils in different stages of development and some intrazonal soils ([dataset] FAO/IIASA/ISRIC/ISSCAS/JRC, 2012). Topographies in the IIA, IIC, IID, IC, and IB geomorphological regions consist of hills with a small elevation range (Zhang, 2002). These topographies influence soil development by soil erosion (Gracheva, 2011). However, an erosion-controlled spatial soil pattern essentially depends on the properties of the parent material (Gracheva, 2011). Accordingly, parent material could have the same importance as topography in influencing the pedodiversity in geomorphological regions IIA, IIC, IC, and IB (Figs. 6a, 7, 8). The landscape in the IID region is a karst landscape (Comprehensive Department National Bureau of Statistics, 2004). Parent material in the karst landscape is mainly limestone. Parent material type determines the degree of soil development in karst landscapes due to the slower development rate of limestone compared with other parent materials (Zhang, 2002; Zhou, 1981). Accordingly, parent material controlled pedodiversity in the IID region. Topographies in the VE, VB, VD, IVB, and IVD geomorphological regions mainly consist of mountains with a large elevation range. Topography influences the variability in soil-forming factors through soil erosion and by influencing climate type (Fu et al., 2018b; Ibáñez and Effland, 2011). Therefore, in geomorphological regions VE, IVB, and IVD, the major controlling factors of pedodiversity were topography (Figs. 6a, 7, 8). The landscapes in the VD and VB geomorphological regions are also karst landscapes (Comprehensive department national bureau of statistics, 2004). Accordingly, parent material mainly controlled the pedodiversity in the two regions (Figs. 6a, 7, 8).

5.3. The effect of the analysis unit size on the study of pedodiversity

Previous studies implied that landscape type may be one of the driving factors of pedodiversity (Dazzi et al., 2009; Papa et al., 2011; Saldaña and Ibáñez, 2004). For example, the main driving factor of diversity in the landscape of fluvial terraces is time (Saldaña and Ibáñez, 2004). However, the driving factor in landscapes with large-scale farming is anthropogenic activity (Dazzi et al., 2009; Papa et al., 2011). A large region could support more landscape types than a small region, which may result in great differences between the main landscape types of the two areas (Ibáñez et al., 2005a). For example, with an increase in the study area, the main landscape types change from plains to mountains. Therefore, the main driving factor of diversity in a large region may be different from that in a small region.

The result of the major controlling factors of diversity based on first-order geomorphological regions showed that the major controlling factor in China, except the Qinghai-Tibetan Plateau, was parent material, which was different from that based on the second-order geomorphological regions (Figs. 6a, 7, 8). The reason for the difference may be that the area of each region in the first-order geomorphological regions was significantly larger than that in the second-order geomorphological regions (Wang et al., 2020). The former supported a larger area of alluvial and aeolian landscapes or karst landscapes than the latter, which may lead to a significant difference in the main landscape types between the two (Liu and Yuan, 1985). The difference also suggested that the size of an analysis unit influenced the analysis result of the driving factor of diversity.

6. Conclusions

Based on the first-order geomorphological regions and second-order geomorphological regions, the effects of the size of analysis unit on spatial distribution characters of pedodiversity and its major driving factor in China were analyzed using a combined approach of moving windows and geographical detector.

The results showed that pedodiversity was highest in southern China with complex terrain, sufficient precipitation and temperature, followed by northern China with relatively flat terrain and insufficient precipitation and was lowest in the Qinghai-Tibet Plateau, which had an extreme soil-forming environment. The regularity of the spatial distribution pattern of pedodiversity based on the two levels of geomorphological regions was similar, which indicated that the analysis unit sizes had little effect on the study on spatial distribution pattern of pedodiversity. The major driving factor analysis of pedodiversity based on first-order geomorphological regions showed that the major driving factor in

China, except for the Qinghai-Tibet Plateau, was parent material. However, the results based on second-order geomorphological regions showed that the major driving factors of pedodiversity, except for the Qinghai-Tibet Plateau, were parent material and topography in hilly regions, topography in mountainous regions, and parent material in regions occupied by alluvial landforms, aeolian landforms, or karst landforms. The driving factor analysis of pedodiversity based on the two levels of geomorphological regions suggested that the effect of the analysis unit sizes on the major driving factor study was significant. The results of this study are an important supplement for pedodiversity studies and provide valuable information for the conservation and management of soil resources in China.

Declaration of Competing Interest

The authors declare that they have no known competing financial interests or personal relationships that could have appeared to influence the work reported in this paper.

Acknowledgments

This work was supported by the National Natural Science Foundation of China (41877071; 42077065).

References

Amundson, R., Berhe, A.A., Hopmans, J.W., Olson, C., Sztein, A.E., Sparks, D.L., 2015. Soil and human security in the 21st century. Science. 348, 1261071. https://doi.org/10.1126/science.1261071.

Amundson, R., Guo, Y., Gong, P., 2003. Soil Diversity and Land Use in the United States. Ecosystems 6 (5), 470–482. https://doi.org/10.1007/s10021-002-0160-2.

Behrens, T., Schneider, O., Lösel, G., Scholten, T., Hennings, V., Felix-Henningsen, P., Hartwich, R., 2009. Analysis on pedodiversity and spatial subset representativity-the German soil map 1:1,000,000. J. Plant. Nutr. Soil. SC. 172 (1), 91–100. https://doi.org/10.1002/jpln.v172:110.1002/jpln.200700339.

Chen, H.Z., Gao, Y.X., Wu, Z.D., 1981. The influence of plateau uplift on the formation of alpine soil in Qing Hai-Tibet region. Acta Pedological Sinica 8, 137–147 (in Chinese).

Comprehensive department national bureau of statistics, 2004. China statistical yearbook for regional economy. Chinese Financial and Economic Publishing House, Beijing (in Chinese).

Daněk, P., Šamonil, P., Phillips, J.D., 2016. Geomorphic controls of soil spatial complexity in a primeval mountain forest in the Czech Republic. Geomorphology 273, 280–291. https://doi.org/10.1016/j.geomorph.2016.08.023.

Dazzi, C., Papa, G.L., Palermo, V., 2009. Proposal for a new diagnostic horizon for WRB Anthrosols. Geoderma 151 (1–2), 16–21. https://doi.org/10.1016/j.geoderma.2009.03.013.

Dazzi, C., Giuseppe, L.P., 2016. Taxonomic and environmental implication of pedotechnique in large scale farming. Int. Soil Water Conse. 4 (2), 137–141. https://doi.org/10.1016/j.iswcr.2016.01.001.

Editorial Committee of geomorphological Atlas of the people's Republic of China, 2009. The geomorphological atlas of the people's republic of China (1:1 million). Science Press, Beijing.

FAO/IIASA/ISRIC/ISSCAS/JRC, 2012. Harmonized World Soil Database (version 1.2). https://webarchive.iiasa.ac.at/Research/LUC/External-World-soil/database/HTML/HWSD_ html?sb=4.

FAO/Unesco, 1997. Soil map of the world (revised legend with corrections and updates). ISRIC, Wageningen, Rome.

Forman, R.T.T., 1995. Land mosaics. The ecology of landscapes and regions. Cambridge Univ. Press, Cambridge. 632 pp.

Fu, T.G., Han, L.P., Gao, H., Liang, H.Z. Liu, J.T. 2018a. Geostatistical analysis of pedodiversity in Taihang Mountain region in North China. Geoderma. 328, 91-99. https://doi.org/ 10.1016/j.geoderma.2018.05.010.

Fu, T.G., Han, L.P., Gao, H., Liang, H.Z., Li, X.H., Liu, J.T., 2018b. Pedodiversity and its controlling factors in mountain regions — A case study of Taihang Mountain. China. Geoderma. 310, 230–237. https://doi.org/10.1016/j.geoderma.2017.09.027.

Fu, T., Han, L., Gao, H., Liang, H., Liu, J., 2019. Rare and endangered soils in the Taihang Mountain region, North China. Land. Degrad. Dev. 30 (14), 1739–1750. https://doi.org/10.1002/ldr.v30.1410.1002/ldr.3381.

Gerasimova, M.I., Golovleva, I.A., Konyushkova, M.V., Sorokin, A.S., Krasilnikov, P.V. 2020. Assessment of soil diversity using soil maps with different scales in Eastern Fennoscandia, Russia. Geoderma Reg. 21, e00274. https://doi.org/ 10.1016/j.geodrs.2020. e00274.

Gao, X., Cheng, W., Wang, N., Liu, Q., Ma, T., Chen, Y., Zhou, C., 2019. Spatio-temporal distribution and transformation of cropland in geomorphologic regions of China during 1990–2015. J. Geogr. Sci. 29 (2), 180–196. https://doi.org/10.1007/s11442-019-1591-4.

Gong, Z.T., Zhang, G.L., Chen, Z.C., 2007. Pedogenesis and soil taxonomy. Science Press, Beijing (in Chinese).

Gracheva, R., 2011. Formation of soil diversity in the mountainous tropics and subtropics: Rocks, time, and erosion. Geomorphology 135 (3-4), 224–231. https://doi.org/10.1016/j.geomorph.2011.02.008.

Ibáñez, J.J., Caniego, J., García-Álvarez, A. 2005a. Nested subset analysis and taxa-range size distributions of pedological assemblages: implications for biodiversity studies. Ecol. Model. 182, 239-256. https://doi.org/10.1016/j.ecolmodel.2004.04.004.

Ibáñez, J.J., Caniego, J., San José, F., Carrera, C., 2005b. Pedodiversity-area relationships for islands. Ecol. Model. 182 (3-4), 257–269. https://doi.org/10.1016/j.ecolmodel.2004.04.005.

Ibáñez, J.J., De-Alba, S., Lobo, A., Zucarello, V., 1998. Pedodiversity and global soil patterns at coarse scales (with discussion). Geoderma 83 (3-4), 171–192. https://doi.org/10.1016/S0016-7061(97)00147-X.

Ibán'ez, J.J., De-Albs, S., Bermúdez, F.F., García-Álvarez, A., 1995. Pedodiversity: concepts and measures. Catena. 24 (3), 215–232. https://doi.org/10.1016/0341-8162(95)00028-Q.

Ibánez, J.J., Feoli, E. 2013. Global relationships of pedodiversity and biodiversity. Vadose Zone J. 12(3), 1-5. http://doi.org/J. 10.2136/vzj2012.0186.

Ibáñez, J.-J., Effland, W.R., 2011. Toward a Theory of Island Pedogeography: testing the driving forces for pedological assemblages in archipelagos of different origins. Geomorphology 135 (3-4), 215–223. https://doi.org/10.1016/j.geomorph.2011.02.010.

Ibáñez, J.J., Pérez-Gómez, R., Oyonarte, C., Brevik, E.C., 2015. Are there arid land soilscapes in Southwestern Europe? Land Degrad Dev. 26 (8), 853–862. https://doi.org/10.1002/ldr.2451.

Ibáñez, J.J., Zuccarello, V., Ganis, P., Feoli, E. 2014. Pedodiversity deserves attention in plant biodiversity research. Plant. Biosyst. 148, 1112-1116. http://doi.org/10.1080/11263504.2014.980357.

Kong, W.J., Xia, H.J., Zhang, Y., 2016. Minimum sampling area for the monitoring of herb diversity in riparian zone of temperate rivers. China. Ecol Res 31 (4), 547–555. https://doi.org/10.1007/s11284-016-1363-x.

Li, B., Pan, B., Cheng, W., Han, J., Qi, D., Zhu, C., 2013. Research on geomorphological regionalization of China. Acta Geogr. Sinica. 68, 291–306 (in Chinese).

Li, B.Y., Pan, B.T., Han, J.F., 2008. Basic terrestrial geomorphological types in China and their circumscriptions. Quaternary Sci. 4(28), 535-543. (in Chinese).

Liu, C.R., Ma, K.P., Yu, S.L., Wang, W., 1998. Plant community diversity in Dongling Mountain, Beijing, China—the determination of critical sampling areas for several types of plant communities. Acta Ecol Sin 18, 15–23 (in Chinese).

Liu, D.S., Yuan, B.Y., 1985. Eolian process and dust mantle (loess) in China. Quaternary Sci. 1, 113–125 (in Chinese).

Lo Papa, G., Palermo, V., Dazzi, C., 2011. Is land-use change a cause of loss of pedodiversity? The case of the Mazzarrone study area, Sicily. Geomorphology 135 (3-4), 332–342. https://doi.org/10.1016/j.geomorph.2011.02.015.

McBratney, A.B., 1992. On variation, uncertainty and informatics in environmental soil-management. Aust. J. Soil. Res. 30, 913–935. https://doi.org/10.1071/SR9920913.

McBratney, A., Minasny, B., 2007. On measuring pedodiversity. Geoderma 141 (1-2), 149–154. https://doi.org/10.1016/j.geoderma.2007.05.012.

Minasny, B., McBratney, A.B., Hartemink, A.E., 2010. Global pedodiversity, taxonomic distance, and the World Reference Base. Geoderma 155 (3-4), 132–139. https://doi.org/10.1016/j.geoderma.2009.04.024.

Palmer, M.W., 1990. The estimation of species richness by extrapolation. Ecology 71 (3), 1195–1198.

Pindral, S., Kot, R., Hulisz, P., Charzyński, P. 2020. Landscape metrics as a tool for analysis of urban pedodiversity. Land. Degrad. Dev. 31, 2281-2294. https://doi.org/10.1002/ldr.3601.

Rannik, K., Kõlli, R., Kukk, L., Fullen, M.A., 2016. Pedodiversity of three experimental stations in Estonia. Geoderma. Reg. 7 (3), 293–299. https://doi.org/10.1016/j.geodrs.2016.05.002.

Ren, J.S., Wang, Z.X., Chen, B.W., 1999. The tectonics of China from a global view: a guide to the tectonic map of China and adjacent regions. Geological Publishing House, Beijing (in Chinese).

Saldaña, A., Ibáñez, J.J., 2004. Pedodiversity analysis at large scales: an example of three fluvial terraces of the Henares River (central Spain). Geomorphology 62 (1-2), 123–138. https://doi.org/10.1016/j.geomorph.2004.02.007.

Shangguan, W., Gong, P., Liang, L., Dai, Y., Zhang, K., 2014. Soil diversity as affected by land use in China: consequences for soil protection. Sci. World. J. 2014, 1–12. https://doi.org/10.1155/2014/913852.

Shi, X.Z., Yu, D.S., Xu, S.X., Warner, E.D., Wang, H.J., Sun, W.X., Zhao, Y.C., Gong, Z.T., 2010. Cross-reference for relating Genetic Soil Classification of China with WRB at different scales. Geoderma 155 (3-4), 344–350. https://doi.org/10.1016/j.geoderma.2009.12.017.

Shi, X.Z., Yu, D.S., Yang, G.X., Wang, H.J., Sun, W.X., Du, G.H., Gong, Z.T., 2006. Cross-reference benchmarks for translating the genetic soil classification of china into the Chinese soil taxonomy. Pedosphere. 16 (2), 147–153. https://doi.org/10.1016/S1002-0160(06)60037-4.

Simonson, R.W., 1959. Outline of a generalized theory of soil genesis. Soil. Sci. Soc. Am. J. 23 (2), 152–156. https://doi.org/10.2136/sssaj1959.03615995002300020021x.

Tazikeh, H., Khormali, F., Amini, A., Motlagh, M.B., Ayoubi, S., 2017. Soil-parent material relationship in a mountainous arid area of Kopet Dagh basin, North East Iran. Catena. 152, 252–267. https://doi.org/10.1016/j.catena.2017.01.020.

Wang, N., Cheng, W., Wang, B., Liu, Q., Zhou, C., 2020. Geomorphological regionalization theory system and division methodology of China. J. Geogr. Sci. 30 (2), 212–232. https://doi.org/10.1007/s11442-020-1724-9.

Wang, J., Li, X., Christakos, G., Liao, Y., Zhang, T., Gu, X., Zheng, X., 2010. Geographical detectors-based health risk assessment and its application in the neural tube defects study of the heshun region, China. Int. J. Geogr. Inf. Sci. 24 (1), 107–127. https://doi.org/10.1080/13658810802443457.

Wilson, M.J., 2019. The importance of parent material in soil classification: A review in a historical context. Catena. 182, 104131. https://doi.org/10.1016/j.catena.2019.104131.

Wu, D.S., Gong, Z.T., 1983. The principal component analysis of soil geochemical types in the tropical and subtropical China. Acta Geogr. Sinica. 20, 431–439 (in Chinese).

Wu, Z. Y. 1995. Vegetation in China. Science Press, Beijing. (in Chinese).

Yu, P., Xu, H., Liu, S., Qiao, M., Zhang, Q., An, H., Fu, J., 2011. Spatial distribution pattern changes of oasis soil types in Manasi River Basin, arid northwestern China. Catena. 87 (2), 253–259. https://doi.org/10.1016/j.catena.2011.06.001.

Zhang, B.P., 2019. Ten major scientific issues concerning the study of China's north-south transitional zone. Prog. Geogr. (in Chinese).

Zhang, F.R., 2002. Soil geography. China Agriculture Press, Beijing (in Chinese).

Zhou, G.C., 1981. The characteristics of soil genesis and the regularity of soil distribution in Guizhou province. Acta Geogr. Sinica 18, 11–23 (in Chinese).

Zinck, J.A., 2013. Geopedology. Elements of geomorphology for soil and geohazard studies, ITC special lecture note series. ITC, Enschede.